THE ASTROPHYSICAL JOURNAL, 423:207–222, 1994 March 1

RAM-PRESSURE STRIPPING OF GAS FROM COMPANIONS AND ACCRETION ONTO A SPIRAL GALAXY: A GASEOUS MERGER

YOSHIAKI SOFUE
Institute of Astronomy, University of Tokyo, Mitaka, Tokyo 181, Japan
Received 1993 July 2; accepted 1993 September 13

ABSTRACT

We simulated the behavior of interstellar gas clouds in a companion galaxy during a gasdynamical interaction with the halo and disk of a spiral galaxy. Due to the ram pressure, the gas clouds are stripped from the companion and accreted toward the disk of the spiral galaxy. If the companion's orbit is retrograde with respect to the rotation of the spiral galaxy, infalling clouds hit the nuclear region. Angular momentum transfer causes disruption of the inner gaseous disk and makes a void of interstellar gas in the bulge. If the companion's orbit is either prograde or polar, infalling clouds are accreted by the outer disk and form a rotating gas ring. We show that the ram-pressure stripping and accretion is one way from the companion to a gas-rich larger galaxy, which causes disposal of interstellar gas from the companion and effectively changes its galaxy type into an earlier (redder) type. The ram-pressure process is significant during the merger of galaxies, in which interstellar gas is stripped and accreted prior to the stellar body merger.

Based on the simulation, we discuss a possible history of interstellar gas in the M31 system, which comprises M32, NGC 205, and possible merged galaxies. The ram-pressure stripping explains the disposal of mass lost from evolving stars in the dwarf elliptical companion M32. The peculiar "face-on" spirals of ionized gas and dark clouds observed in M31's bulge can be reproduced by a spiral inflow of accreting gas from the companions and/or from the merger galaxy.

Subject headings: accretion, accretion disks — galaxies: individual (M31, M32, NGC 205) — galaxies: interactions — galaxies: ISM

1. INTRODUCTION

Ram-pressure accretion of intergalactic clouds by galaxies with extended gaseous halos has been studied by numerical simulations, and it was shown that gaseous debris from tidally disrupted galaxies are soon accreted by an encountering galaxy (Sofue & Wakamatsu 1991, 1992, 1993). Observations of a considerable number of early-type galaxies, where gas is moving perpendicularly or in a counterrotating sense to the stellar rotation, have suggested that the acquistion of gas from outside is not a rare event, and sources of such cool gas may be either tidal debris of disturbed galaxies or intergalactic clouds (Sofue & Wakamatsu 1993). On the other hand, ram-pressure stripping of interstellar matter by intergalactic gas has been studied in relation to the origin of S0 galaxies (e.g., Farouki & Shapiro 1980).

Tidal interaction between galaxies has been extensively simulated numerically by the test-particle method (e.g., Toomre & Toomre 1972). Even such a gaseous phenomenon as the Magellanic Stream (Mathewson et al. 1979) has been modeled by a tidal debris from the Magellanic Clouds based on a gravitational test-particle simulation (Fujimoto & Sofue 1976, 1977; Murai & Fujimoto 1980). Merging of galaxies has been studied by taking into account the dynamical friction (Tremaine 1976; Byrd 1979; Murai & Fujimoto 1980), and recent N-body simulations of self-gravitating bodies showed more details of the merging process among galaxies (e.g., Barnes 1989). In these simulations, however, little attention has been paid to the gaseous constituents, which must behave quite differently from stars for its viscous and noncollisionless characteristics.

The giant Sb galaxy M31 and its companions (M32 and NGC 205) provide us a unique opportunity to investigate tidal interaction among galaxies. M32 is an anomalously compact elliptical, known for its tidal cutoff and steep central condensation, which is likely due to a tidal interaction with the M31's disk (Kormendy 1987; Nieto & Prugniel 1987). NGC 205 is a dwarf elliptical with less concentration and is known for its gaseous content and star-forming activity near the center (Johnson & Gottesman 1983; Price & Grasdalen 1983; Bica, Alloin, & Schmidt 1990). Tidal interaction of the companions with M31 has been numerically simulated (Byrd 1976, 1977, 1978; Sato & Sawa 1986), but no attention has been paid to gaseous component and its hydrodynamical behaviour. Recent observations by the *Hubble Space Telescope* discovered a multiple nucleus in M31, which gives definite proof of the merger of substantial galaxies with M31 (Lauer et al. 1993). The central region of M31 exhibits a void of neutral as well as molecular hydrogen gases (e.g., Brinks & Shane 1984; Koper 1990; Sofue & Yoshida 1993): M31 has no nuclear gas disk, unlike the Milky Way. On the other hand, the M31 bulge exhibits a peculiar "face-on" spiral feature, which is observed both in the Hα line emission (Ciardullo et al. 1988) and in optical dark clouds (Sofue et al. 1994), although the gaseous mass is much smaller compared to that found in our Galaxy. This suggests that the inner gaseous disk of M31 has been disrupted for some reason.

In this paper we simulate the stripping of interstellar matter from a companion galaxy and its accretion onto a disk galaxy by applying the ram-pressure accretion theory presented by Sofue & Wakamatsu (1991, 1992, 1993). Based on results of simulations, we discuss the M31 system and attempt to link the properties observed in the dwarf elliptical companions as well as the suggested merger galaxy to the peculiar morphology of gases observed in the central region of M31.

2. RAM-PRESSURE ACCRETION MODEL AND BASIC ASSUMPTION

2.1. H I *and Molecular Clouds*

In this work, we treat ballistic orbits of interstellar gas clouds such as giant molecular clouds, which are initially distributed in companion galaxies with random motion. We assume that individual clouds are gravitationally bound. H I clouds are easily stripped, but they can remain as clouds only when they are massive enough, while less massive clouds are dissipated into the intergalactic space. In this paper, H I clouds are assumed to have dimensions massive enough to be gravitationally bound as the following: radius $R \sim 500$ pc; density $\rho_{\rm H\,I} \sim 1\ m_{\rm H}\ {\rm cm}^{-3}$; and mass $m_{\rm H\,I} \sim 3.05 \times 10^6\ M_\odot$. The H I cloud is gravitationally balanced with its internal motion (or rotation) of $\sigma_{\rm H\,I} = 5.11\ {\rm km\ s}^{-1}$. For a molecular cloud, we assume a size and mass of the same order as those of typical giant molecular clouds in our Galaxy: radius $R \sim 30$ pc; mean density $\rho_{\rm cloud} \sim 10^2\ {\rm H_2\ cm}^{-3}$; and mass $m_{\rm cloud} \sim 1.32 \times 10^5\ M_\odot$. The cloud is assumed to be gravitationally balancing with its internal velocity dispersion of $\sigma_{\rm cloud} = 4.36\ {\rm km\ s}^{-1}$. Alternatively, the cloud may be maintained by rotation of the same amount of velocity.

Although the cloud properties would vary due to interaction with the halo and intergalactic gas, we here simply assume that their original properties are kept during simulation. We make only the following comment: the internal motion of clouds, such as turbulence, would be dissipated, which would cause collapse of the cloud. However, instabilities on the cloud surface due to interaction with the intergalactic gas, such as the Kelvin-Helmholtz instability, would excite and act to maintain the internal motion.

2.2. *Equations of Motion and Potentials of the Galaxies*

We adopt a simple ballistic model, as it has been adopted by Sofue & Wakamatsu (1993) and Farouki & Shapiro (1980). The ram-pressure (dynamical pressure) force on an intergalactic gas cloud (test cloud) is given by $-\pi R^2 \rho(r) \Delta v^2$, where $\Delta \boldsymbol{v} = \boldsymbol{v} - \boldsymbol{V}$ is the relative velocity of a cloud with respect to the halo gas which is rotating at a velocity $\boldsymbol{V}$ in the potential of the disk galaxy, and $\rho(r)$ is the density of diffuse gas distributed around the galaxy, which includes the intergalactic diffuse gas and the halo gas of the galaxy. The equation of motion for a test cloud which was initially distributed in the companion galaxy can be written as

$$\frac{d^2\boldsymbol{r}}{dt^2} = \sum_{j=1}^{2} \frac{\partial \Phi_j}{\partial \boldsymbol{r}} - \frac{3\rho(r)}{4R\rho_c} \Delta v \Delta \boldsymbol{v}\ , \tag{1}$$

where $\boldsymbol{v} = d\boldsymbol{r}/dt$ and $\boldsymbol{r} = (x, y, z)$ are the cloud's velocity and position with respect to the center of the disk galaxy, and ρ_c is the density of the cloud. Here Φ_i are the gravitational potentials for the major galaxy ($j = 1$) and the companion galaxy ($j = 2$). The gravitational potential of the major galaxy is approximated by a modified Miyamoto & Nagai's (1975) potential:

$$\Phi_1 = \sum_{i=1}^{3} \frac{GM_i}{\{\varpi^2 + [a_i + (z^2 + b_i^2)^{1/2}]^2\}^{1/2}}\ , \tag{2}$$

where $\varpi = (x^2 + y^2)^{1/2}$; and M_i, a_i, and b_i are the masses and scale radii for the ith mass component of the galaxy. For the disk galaxy we assume three mass components: a central bulge ($i = 1$); disk ($i = 2$); and a massive halo ($i = 3$). The parameters are given in Table 1.

TABLE 1

PARAMETERS FOR GRAVITATIONAL POTENTIALS

i	Mass Component	$M_i(M_\odot)$	a_i (kpc)	b_i (kpc)
Disk galaxy:[a]				
1	Central bulge	2.05×10^{10}	0	0.495
2	Disk	2.547×10^{11}	7.258	0.520
3	Massive halo	3×10^{11}	20	20
Companion[b]	Spheroid	$M_{\rm C} = 0.1\ M_2$	0	2

[a] Miyamoto-Nagai's 1975 potential with a modified massive halo.

[b] Plummer's potential. As a convenience, we adopted the same parameter for M32 and NGC 205, which little affects the result of accretion after stripping, while the fraction of unstripped molecular clouds would change by different masses.

For the companion galaxy we assume one component, for which $a_1 = 0$, so that the potential represents a Plummer's law:

$$\Phi_2 = \frac{GM_{\rm C}}{\sqrt{r^2 + b_{\rm C}^2}}\ . \tag{3}$$

We assume that the mass of companions is an order of magnitude smaller than the main body of the disk galaxy: $M_{\rm C} = 0.1\ M_2$, and that the center of mass of the system coincides with the center of the major galaxy which is fixed to the origin of the coordinates.

The motion of the companion galaxy is approximated by motion of a test particle rotating around the galaxy in the potential described by equation (2).

The equation of motion of the center of a companion galaxy is written as

$$\frac{d^2\boldsymbol{r}}{dt^2} = \frac{\partial \Phi_1}{\partial \boldsymbol{r}} - kM_{\rm C}\rho_{\rm MH}(r)\frac{\boldsymbol{v}}{v}\ . \tag{4}$$

The second term represents the dynamical friction due to the massive halo, which is assumed to be at rest. The density of the massive halo is assumed to be inversely proportional to the square of r: $\rho_{\rm MH}(r) = \rho_{\rm MH0}(r/100\ {\rm kpc})^{-2}$, with $\rho_{\rm MH0}$ being a constant. The variable k represents the coefficent of the dynamical friction. Although coefficient k is actually a slowly varying function of velocity and mass (Tremaine 1976; Byrd 1979), we here assume it to be constant. We took a value for $k\rho_{\rm MH0}$ so that the acceleration by the second term becomes equal to 0.005 of the gravitational acceleration by the first term when the companion galaxy is at a distance of 100 kpc from the center.

2.3. *Models for Gaseous Disk, Halo, and Intergalactic Gas*

We assume a density distribution of a gaseous halo around the disk galaxy as represented by the following equation:

$$\rho(r) = \rho(\varpi, z) = \rho_0 + \frac{\rho_{\rm H}}{(\varpi/\varpi_{\rm H})^2 + (z/z_{\rm H})^2 + 1} + \frac{\rho_{\rm D}}{(\varpi/\varpi_{\rm D})^2 + (z/z_{\rm D})^2 + 1}\ , \tag{5}$$

where $\rho_{\rm H}$, $\varpi_{\rm H}$, and $z_{\rm H}$ are parameters representing the distribution of halo gas density; $\rho_{\rm D}$, $\varpi_{\rm D}$, and $z_{\rm D}$ are those for the disk component; and ρ_0 is the intergalactic gas density (Sofue & Wakamatsu 1993). Values of the parameters are given in Table 2.

TABLE 2

PARAMETERS FOR GASEOUS COMPONENTS

Parameter	Value
Intergalactic gas:	
ρ_0	$10^{-5}\ m_H\ cm^{-3}$
Halo:	
ρ_H	$0.01\ m_H\ cm^{-3}$
ϖ_H	15 kpc
z_H	10 kpc
Disk:	
ρ_D	$1\ m_H\ cm^{-3}$
ϖ_D	10 kpc
z_D	0.2 kpc
Molecular cloud:	
ρ_{cloud}	$100\ H_2\ cm^{-3}$
R	30 pc
$m = (4\pi/3)R^3\rho_{cloud}$	$1.32 \times 10^5\ M_\odot$
σ_{cloud}	4.36 km s^{-1}
H I cloud:	
$\rho_{H\,I}$	$1\ m_H\ cm^{-3}$
R	500 pc
$m = (4\pi/3)R^3\rho_{H\,I}$	$3.05 \times 10^6\ M_\odot$
$\sigma_{H\,I}$	5.11 km s^{-1}

Since little is known about the rotation of halo gas, we here assume for convenience that the halo gas is rotating around the z-axis with its centrifugal force balancing the galaxy's gravity toward the z-axis:

$$V(\varpi, z) = \left(\sum_{i=1}^{3} \frac{GM_i}{\mu_i^3} \right)^{1/2} \varpi \ . \tag{6}$$

We assume that the gas is in a hydrostatic equilibrium in the z-direction, so that $V_z = 0$, and pressure gradient in the ϖ-direction is neglected. This assumption would be too simplified and the neglection of a pressure gradient in the ϖ-direction may cause an overestimation of the rotation speed of the halo gas.

2.5. *Initial Conditions*

We solve the differential equations by using the Runge-Kutta-Gill method. The time step of integration was taken to be smaller than 0.01 times the dynamical timescale of each test particle (cloud) at the closest approach to the galaxy center. Two cases of initial point of the companions are presented: $(x, y, z) = (0, -100, 100)$ kpc and $(0, -50, 50)$ kpc. Namely, the companions are put at sufficiently distant positions at a latitude of 45° from the galactic plane. Various different initial velocities are given to the companions, usually in the sense that the initial position becomes the apogalactic point. Figure 1 illustrates the coordinate system and the orbit of companion.

N interstellar clouds are initially distributed at random in the companion within a radius R and velocity dispersion σ_v, so that the ensemble of test clouds are maintained to be a spherical system. This might be replaced with a rotating disk of a similar size. However, the initial distribution within the companion have little effect on the accretion process after stripping, and, therefore, we adopt a spherical distribution.

3. SIMULATION AND RESULTS

3.1. *Retrograde Encounter and Polar-Spiral Accretion onto the Nucleus*

Figure 2 shows a result for a 45° inclined retrograde orbit, when the integration started from the apogalacticon at $(x, y, z) = (0, -100, 100)$ kpc at a tangential velocity of $(v_x, v_y, v_z) = (-100, 0, 0)$ km s^{-1}. The upper and lower panels show the (x, z) and (x, y) planes, respectively. The spiral galaxy is rotating counterclockwise in the (x, y) plane.

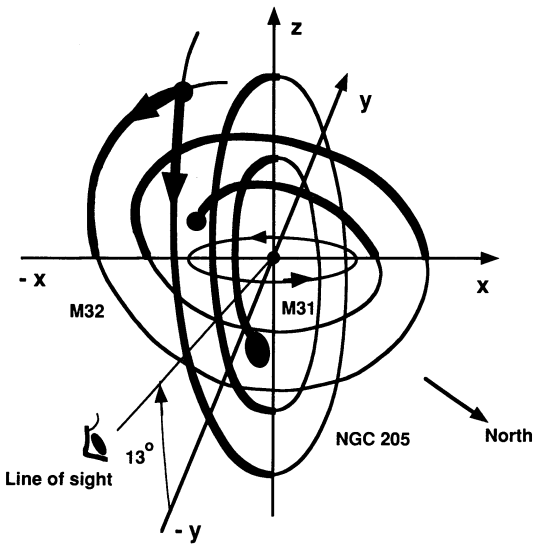

FIG. 1.—Coordinate system and orientation of the disk galaxy with its rotation direction used in the simulation. Possible orbits of M32 and NGC 205 around M31 as discussed in the text and the line of sight are illustrated schematically.

The companion galaxy rotates around the disk galaxy on a semielliptical orbit. Decrease in the apogalactic distance of the companion due to dynamical friction is very gradual and is almost negligible for the present simulation. Orbits of individual gas clouds, which were distributed in the companion, change drastically when they cross the galactic plane, where the clouds suffer from strong ram-braking due to an almost head-on collision with the rotating disk and halo gases. The H I clouds are almost completely stripped from the companion and fall toward the disk of the major galaxy along polar orbits. It is conspicuous that all stripped clouds are finally infalling toward the central region, where they form a polar "accretion" spiral. The clouds are then accreted to the nuclear disk and form a compact disk with a radius of a few kpc.

Stripping of molecular clouds occurs more gently, and many clouds survive the stripping. Accretion of stripped molecular clouds is also slower, and they remain as intergalactic or intrahalo gaseous debris for a longer time than H I clouds, but finally they are accreted by the galaxy.

Figure 3*a* is the same as Figure 2 but for a slower tangential velocity: $v_x = -80$ km s^{-1}. As the perigalactic distance becomes smaller, stronger stripping of H I and also of molecular clouds occurs. Figure 3*b* is the same but for a "final" stage of accretion of the molecular clouds after 8×10^9 yr, about two and one-half orbital rotation. Although the accretion of molecular clouds is slow, they finally infall toward the central region, except for some clouds which survive the stripping and remain in the companion.

Figures 4*a* and 4*c* are the same, but for $v_x = -70$ km s^{-1}, which might simulate M32. Figure 4*b* is an enlargement of Figure 4*a*, which displays the central accretion in more detail. As the encounter with the disk is more direct in the sense of being a head-on collision, the stripping occurs more drastically. The stripped H I clouds infall toward the galaxy center along the accretion spiral and hit the nuclear region. It is inter-

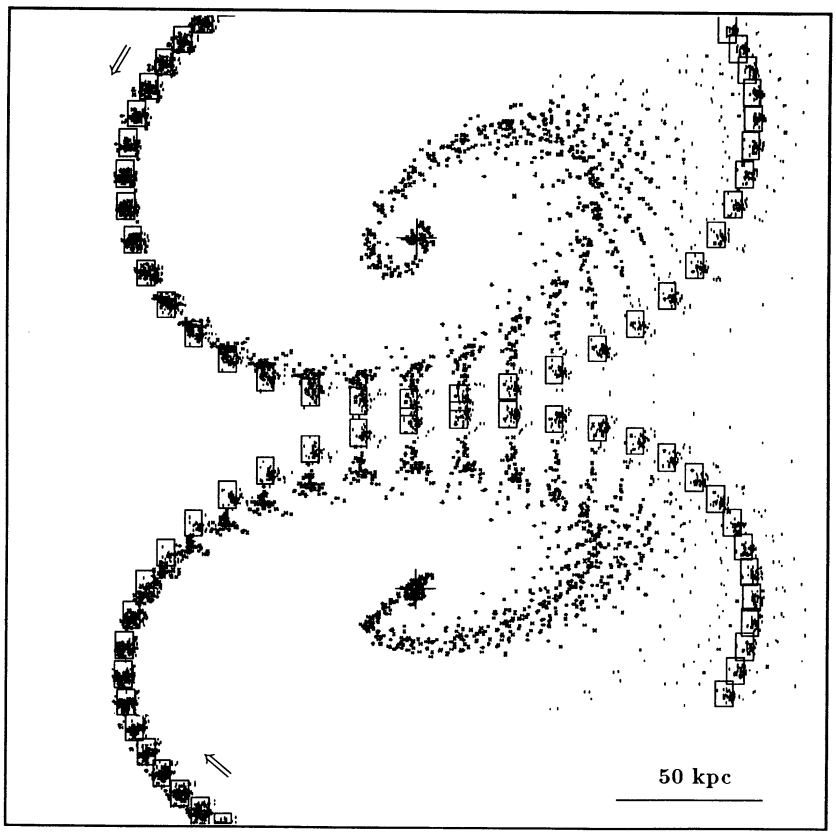

FIG. 2.—Stripping of H I (*asterisks*) and molecular (*dots*) clouds from a companion and their ram-pressure accretion toward M31 for a semiretrograde orbit. The initial condition is $(x, y, z) = (0, -100, 100)$ kpc and $(v_x, v_y, v_z) = (-100, 0, 0)$ km s^{-1}. Upper panel is the projection onto the (x, z) plane (M31 is edge-on), which mimic approximately the view when seen from us, and the lower panel onto (x, y) plane (M31's disk plane). M31 is rotating a counterclockwise on the x, y plane. The cross indicates the center of M31, and the square represents the companion plotted every 0.1 Gyr. Clouds are also plotted every 0.1 Gyr.

esting to examine the tidal effect on the companion's stellar body. Figure 4*d* shows the result of test-particle simulation for the same condition as the cloud but without ram pressure. The star distribution is tidally deformed when the companion passes the perigalactic point, but the effect is significant only in the outer part.

Figure 5 is a case with a smaller distance of the initial position at $(x, y, z) = (0, -50, 50)$ kpc with $(v_x, v_y, v_z) = (-50, 0, -50)$ km s^{-1}. The result is similar to that for Figure 4.

Similar results have been obtained for a wide range of initial conditions of retrograde orbits. Hence, we conclude that, if the companion galaxy approaches the major galaxy on a retrograde orbit, the interstellar gas clouds are stripped, accreted to the central region, and hit the nucleus, within about one revolution period, or a couple of billion years. Such an accretion of gas clouds fuels the nuclear region and may explain the peculiar polar spirals of ionized and molecular gases in the bulge of M31 (Ciardullo et al. 1988; Sofue et al. 1994) (see § 4). It may also have happened that the accretion in the nuclear region triggered a starburst in the center of the disk (Sofue & Wakamatsu 1993).

3.2. *Polar Encounter and Ring Formation*

Figure 6 is the case for an almost polar (overhead) orbit starting from the same initial position as Figure 1 at $(x, y, z) = (0, -100, 100)$ kpc, but for $(v_x, v_y, v_z) = (-20, 50, 50)$ km s^{-1} still in a retrograde sense. The stripping occurs when the companion crosses the galactic plane, and accreting clouds are merged by the rotating disk gas, forming a rotating ring of about 10 kpc.

Figure 7*a* shows a case of a polar encounter for an initial condition, $(x, y, z) = (0, -100, 100)$ kpc and $(v_x, v_y, v_z) = (0, 80, 0)$ km s^{-1}. Figure 7*b* is the result for $(v_x, v_y, v_z) = (0, 0, -80)$ km s^{-1}, which might simulate NGC 205. Figure 7*c* shows a side view of Figure 7*b*. Stripping of H I clouds and their merging with the disk are similar to that shown in Figure 6, and a ring of radius 10 kpc forms. About half of the molecular clouds are stripped, but another half survive the stripping. Such formation of a gaseous ring may be related to the 10 kpc ring of H I and molecular gases in M31 disk (see § 4.).

3.3. *Prograde Encounter and Outer Ring Formation*

Figure 8 is a case of prograde (direct) orbit with the initial position and velocity of $(x, y, z) = (0, -100, 100)$ kpc and $(v_x, v_y, v_z) = (+40, 0, 0)$ km s^{-1}. The stripping is rather mild, because the relative velocity of clouds against the rotating disk and halo is smaller than that in the case of a retrograde encounter. The H I clouds are stripped during the close passage of the galactic plane, and they begin to corotate with the disk gas by the friction and finally attain a ring of radius 15 kpc. In such a prograde accretion, a part of the orbital angular momentum of the infalling clouds will be transferred to that of

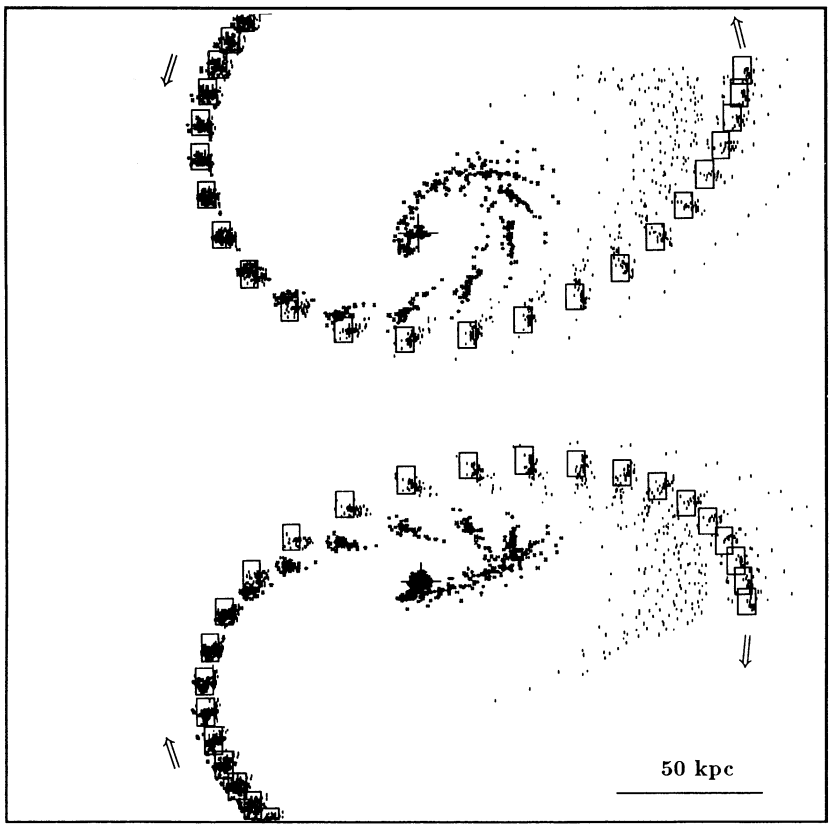

FIG. 3a

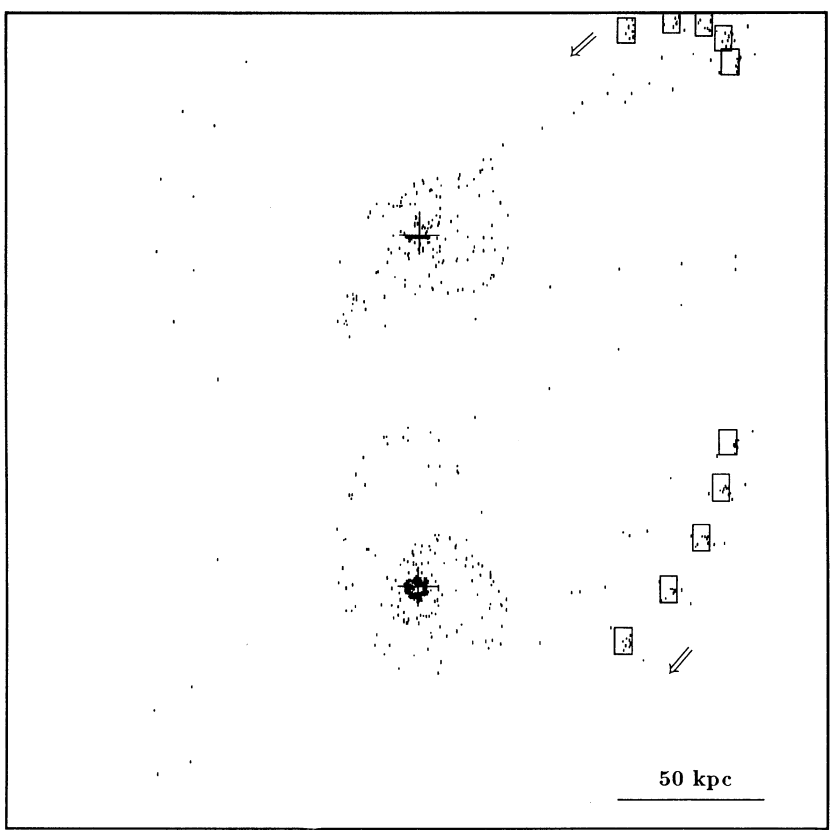

FIG. 3b

FIG. 3.—(*a*) The same as Fig. 2 but for a prograde orbit of the companion. The initial condition is $(x, y, z) = (0, -100, 100)$ kpc and $(v_x, v_y, v_z) = (-80, 0, 0)$ km s^{-1}. (*b*) The same but after 8 Gyr. Molecular clouds are also accreted toward M31's center.

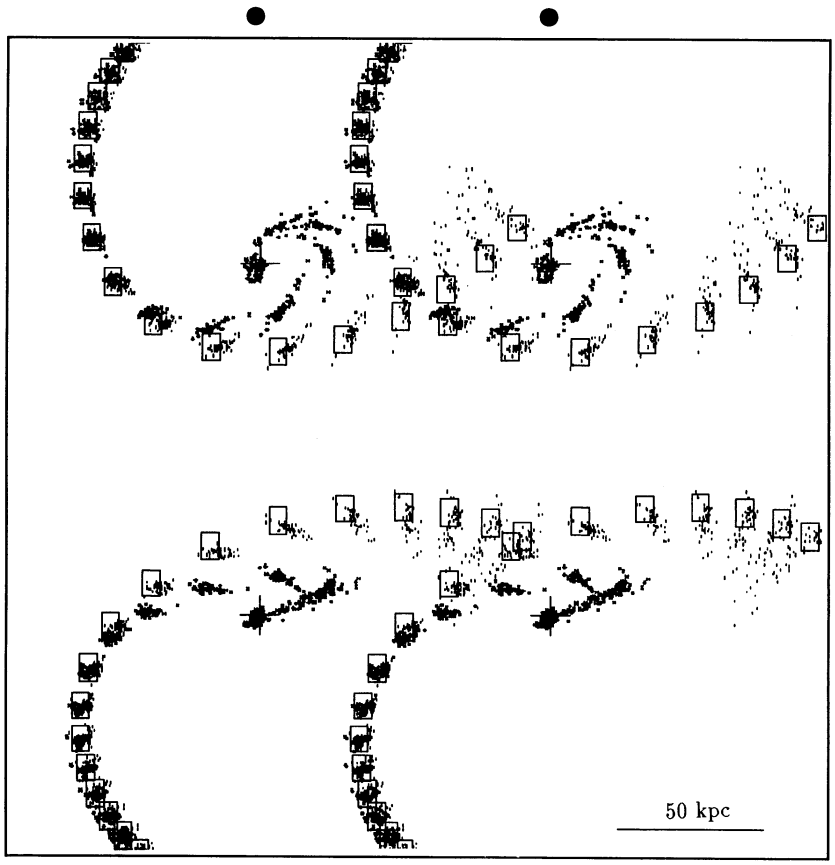

FIG. 4a

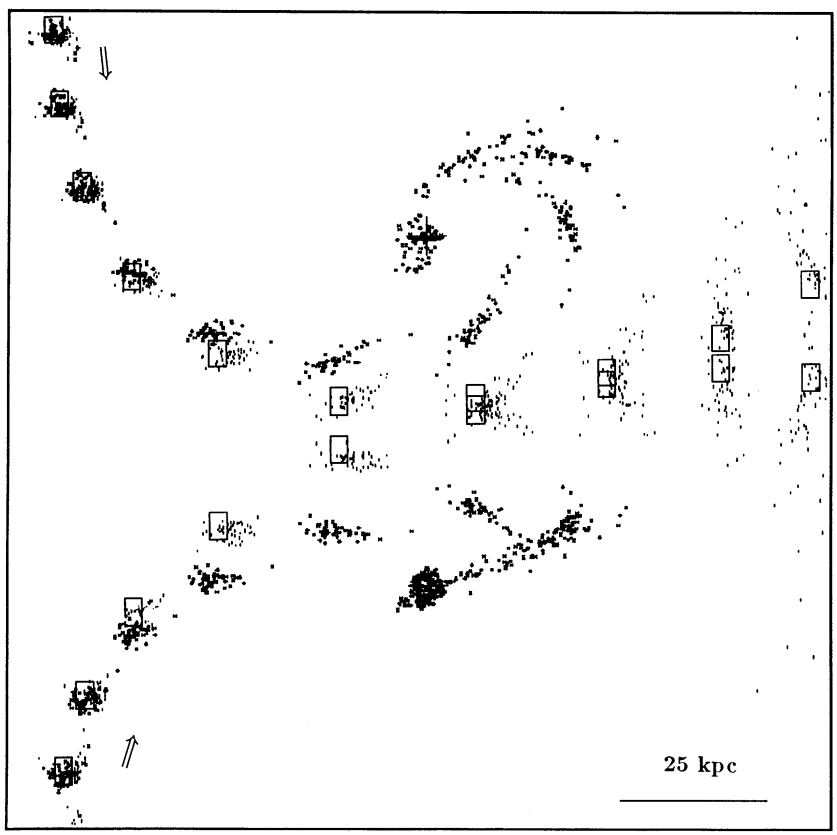

FIG. 4b

FIG. 4.—(*a*) The same as Fig. 2, but for the initial condition $(x, y, z) = (0, -100, 100)$ kpc and $(v_x, v_y, v_z) = (-70, 0, 0)$ km s^{-1}. This case simulates M32. (*b*) Enlargement of (*a*), in order to see the central accretion spirals. The clouds are distributed spirally with a large tilt angle from the galactic plane. This mimics the peculiar "face-on" spiral feature as observed in molecular clouds (Sofue et al. 1994) and in Hα (Ciardullo et al. 1988) as shown in Figs. 11 and 12. Plot interval is 0.1 Gyr. (*c*) The same as (*a*) but until 4 Gyr, plotted every 0.2 Gyr. (*d*) The same as (*c*), but for the stellar component, for which only gravitation has an effect, without ram force.

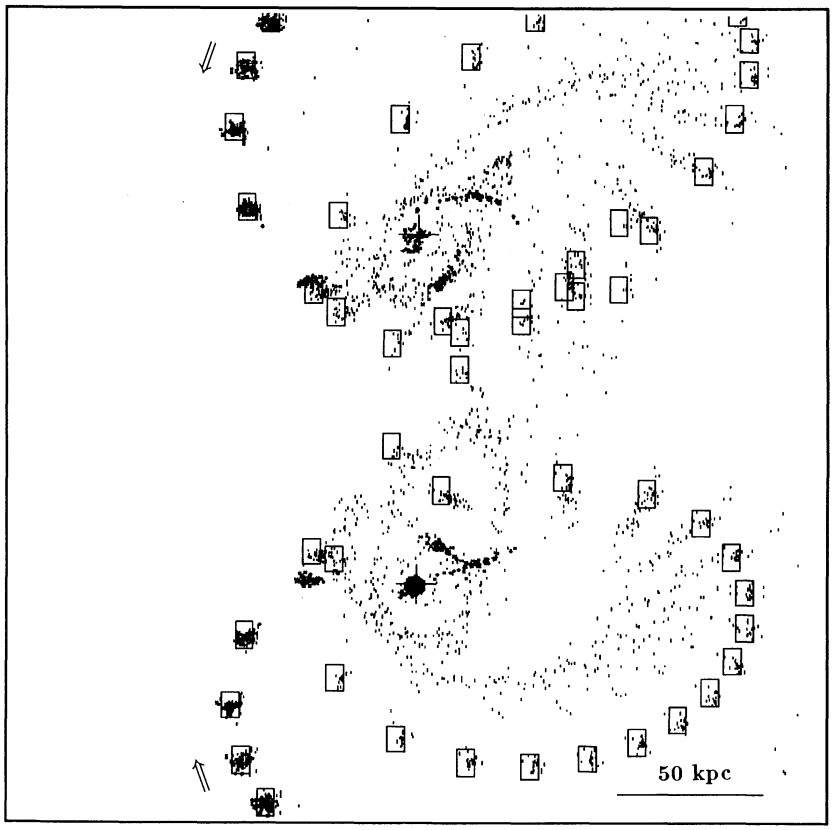

FIG. 4*c*

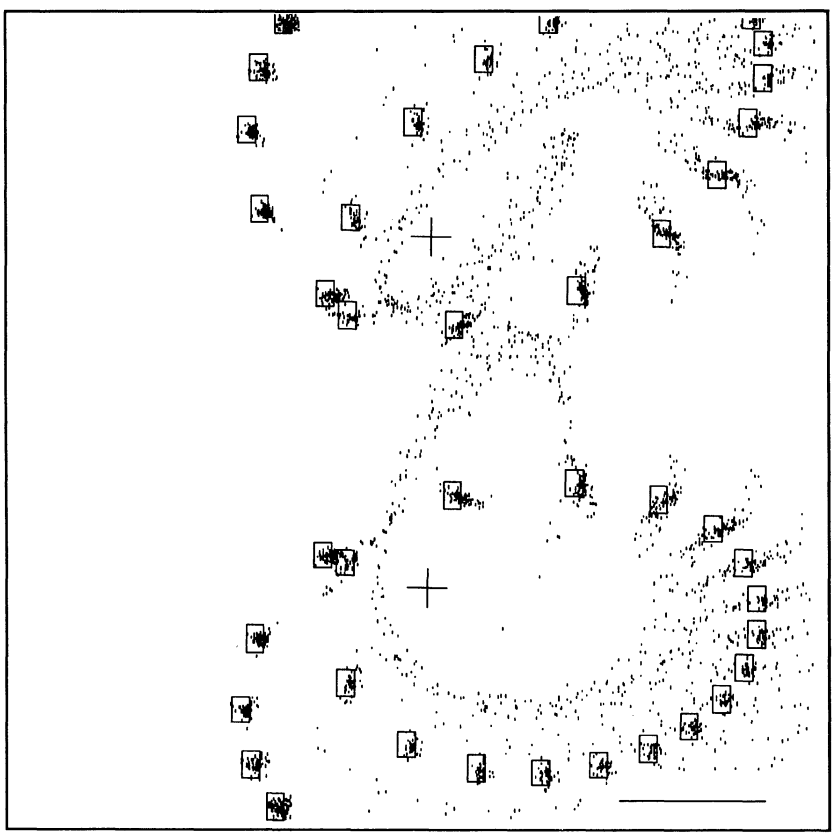

FIG. 4*d*

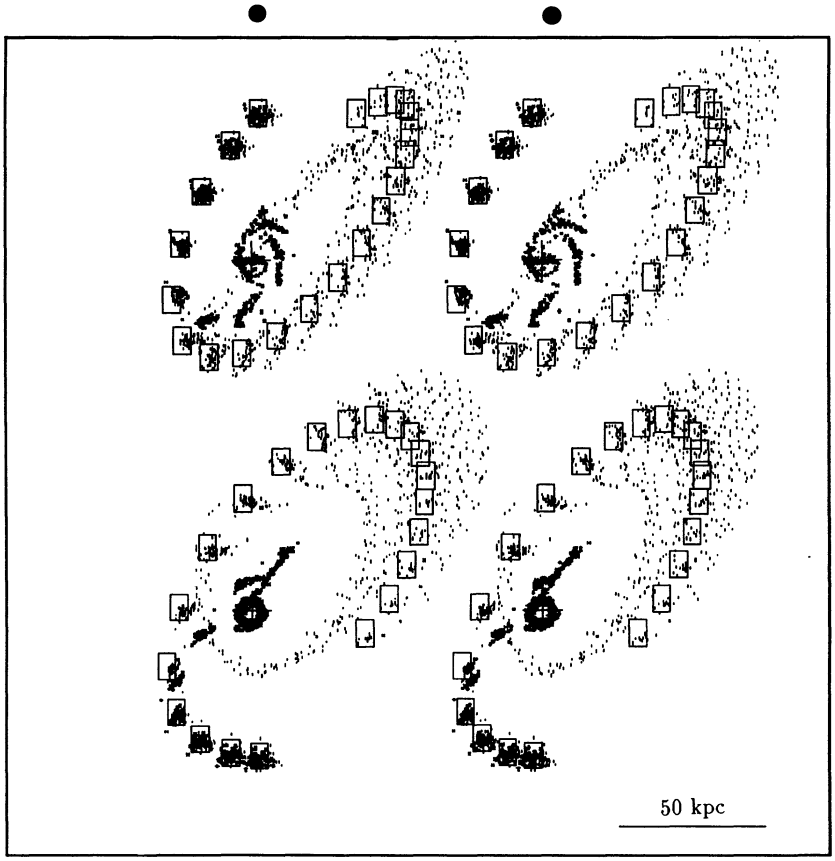

FIG. 5.—The same as Fig. 1, but for a closer orbit with an initial condition $(x, y, z) = (0, -50, 50)$ kpc and $(v_x, v_y, v_z) = (-50, 0, -50)$ km s^{-1}. Plot interval is 0.2 Gyr. The display is a stereogram in order to obtain an impression of the three-dimensional structure of the simulated feature.

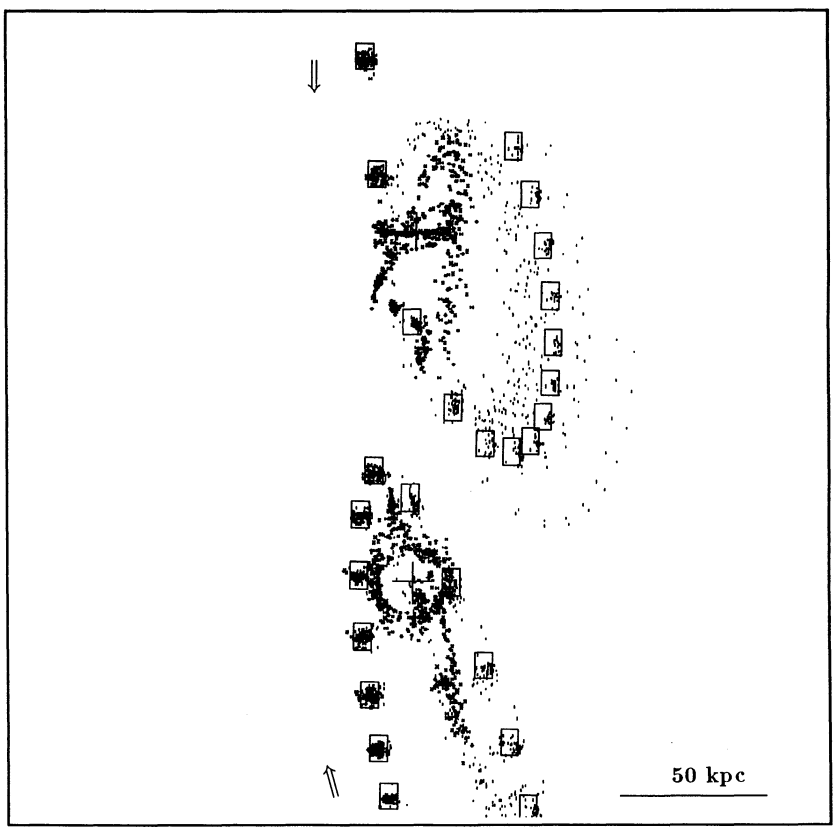

FIG. 6.—The same as Fig. 1, but for a semipolar orbit with an initial condition $(x, y, z) = (0, -100, 100)$ kpc and $(v_x, v_y, v_z) = (-20, 50, 50)$ km s^{-1}. Stripped clouds form a ring of radius 10 kpc. Plot interval is 0.2 Gyr.

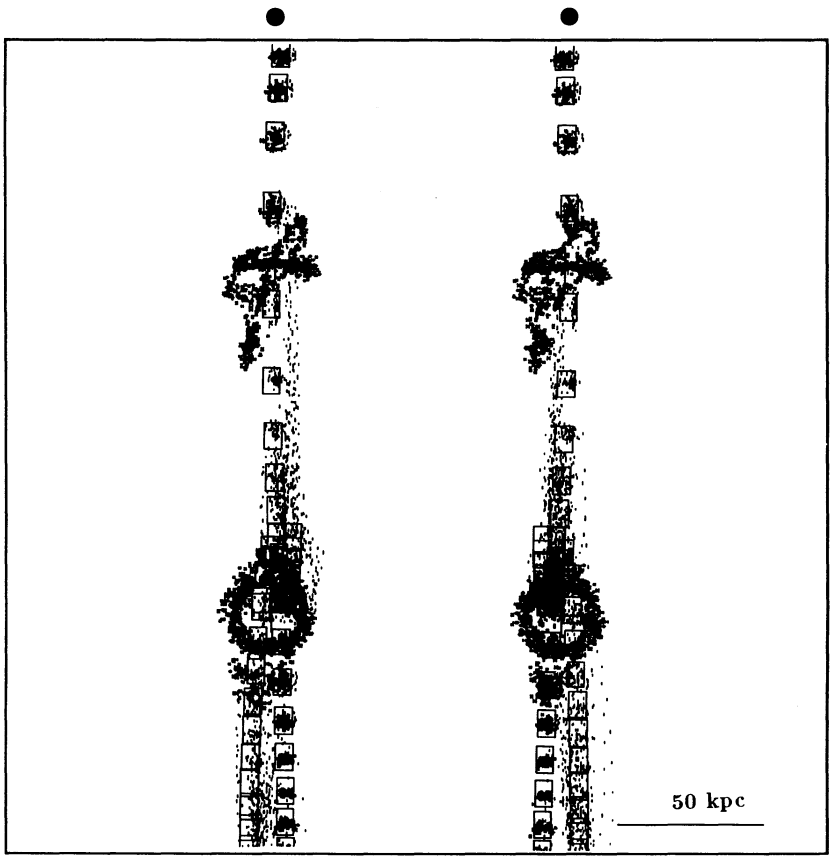

FIG. 7a

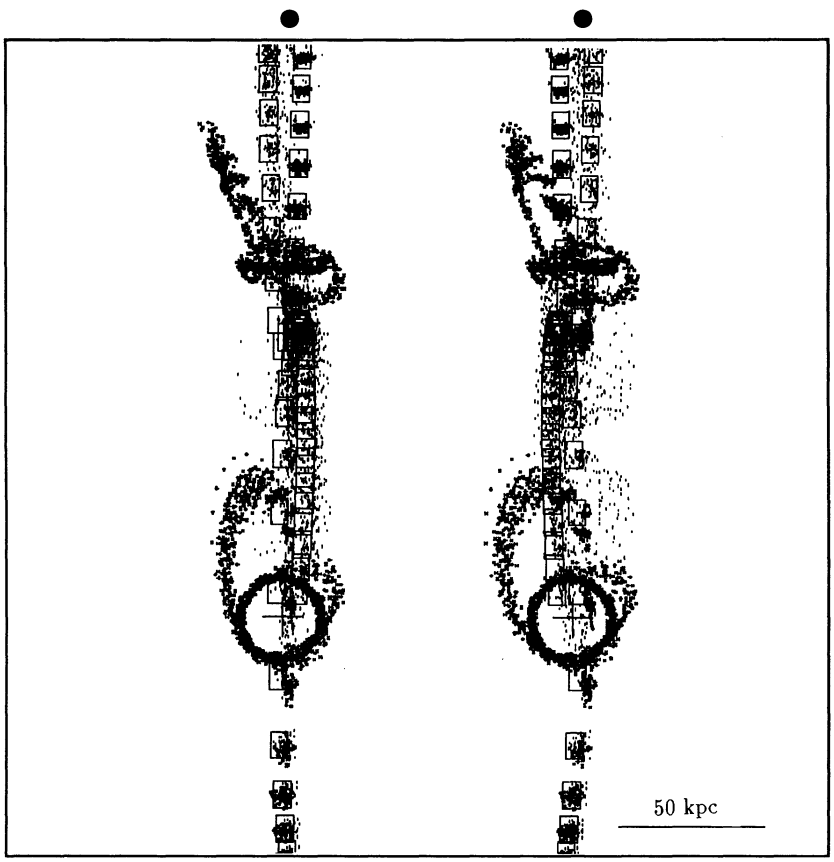

FIG. 7b

FIG. 7.—(*a*) Polar encounter for an initial condition (x, y, z) = (0, −100, 100) kpc and (v_x, v_y, v_z) = (0, 80, 0) km s^{-1}. Stripped clouds form a 10 kpc ring. Plot interval is 0.2 Gyr. The display is a stereogram. (*b*) Polar encounter for an initial condition (x, y, z) = (0, −100, 100) kpc and (v_x, v_y, v_z) = (0, 0, −80) km s^{-1}. This mimics the orbit of NGC 205. The display is a stereogram. (*c*) Side view of (*b*).

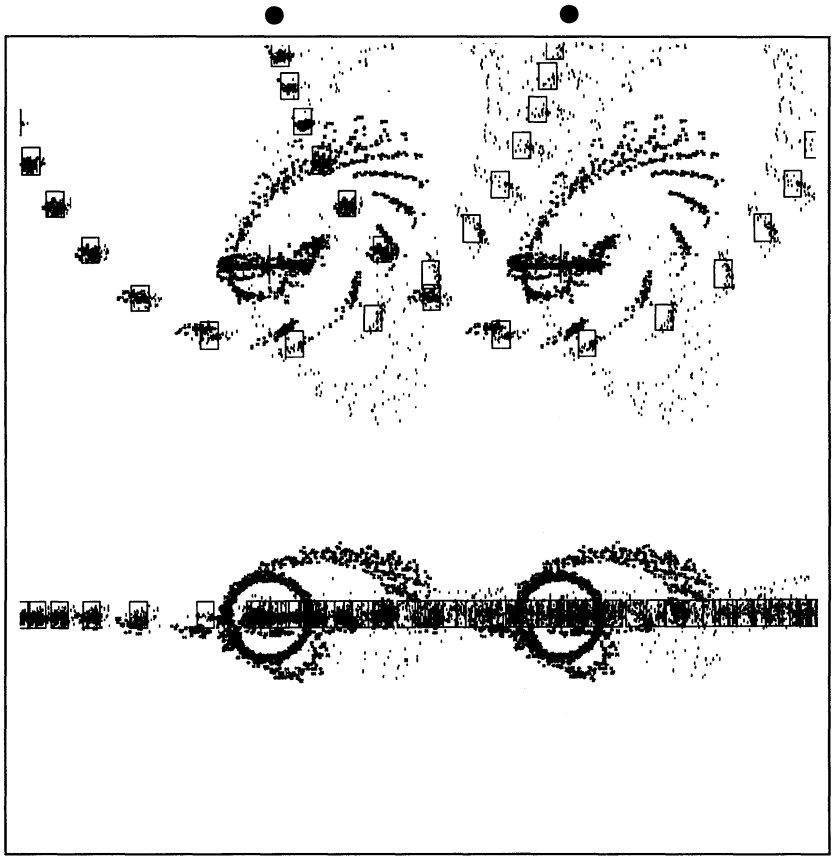

FIG. 7c

disk rotation, increasing the angular momentum of the disk and therefore increasing the disk radius (see § 4).

Figure 9 is the same as Figure 8, but with larger tangential velocity, $v_x = +50$ km s^{-1}. Again a mild stripping of H I clouds and merging by the disk results in the formation of a large radius ring. It is also interesting to observe that outer spiral arms, which are warped from the disk plane, appear during the accretion. On the other hand, only the outer parts of molecular clouds of the companion are stripped, but the inner clouds remain unstripped.

Figure 10 is the case for a closer orbit starting at (0, −50, 50) kpc with (20, 50, 0) km s^{-1}. A similar result is observed: a ring of about 15 kpc radius forms.

4. GASEOUS MERGER IN M31 SYSTEM

4.1. *Orbits and Masses of M32 and NGC 205*

4.1.1. *M32*

Although some suggestions have been made (Byrd 1976, 1977; Sato & Sawa 1986; Cepa & Beckman 1988), no definite orbits for the companions has been determined, as was done for the Magellanic Clouds (Fujimoto & Sofue 1976, 1977). The projected distance of the present position of M32 from M31's center is 21′.4 = 4.2 kpc to the southwest. The measured distance and radial velocity of M31 are 670 kpc and −299 km s^{-1}, respectively, and those of M32 are 660 kpc and −217 km s^{-1} (Allen 1973; de Vaucouleurs et al. 1991). Ford, Jacoby, & Jenner (1978) found M32 to lie in front of M31 from observations of planetary nebulae. From these, we can estimate that M32 is about 10 kpc nearer to us and the galactocentric distance of about 11 kpc. This is consistent with the difference in distance to M32 and the M31 nucleus of 7.5 kpc as concluded by Byrd (1976).

M32 is approaching toward M31 at a relative line-of-sight velocity of +82 km s^{-1}. The disk of M31 is rotating at a velocity of 220 km s^{-1} in the sense that the southwest side, where the projected M32 is located, is approaching us. Therefore, the line-of-sight velocity of M32 is retrograde with respect to M31's rotation. From the geometry of the two galaxies, the probability of retrograde orbit is 63%. We may thus suppose that M32 is rotating around M31 in a retrograde sense. In this case M32's orbit and stripping and accretion process would be simulated by the results in Figures 4 and 5. Cepa & Beckman (1988) also suggested that M32's orbit is retrograde, while they assumed that M32 is located farther than M31 and its present position is almost in the disk of M31, which appears to be inconsistent with the observations by Ford et al. (1978). Byrd (1976) took an opposite rotation based on a tidal warping model of the H I disk, while parameters like the mass of M32 were taken to be much larger than the recently determine value, so that the orbit determination must be reviewed.

Obviously, the present position of M32 is too close to M31

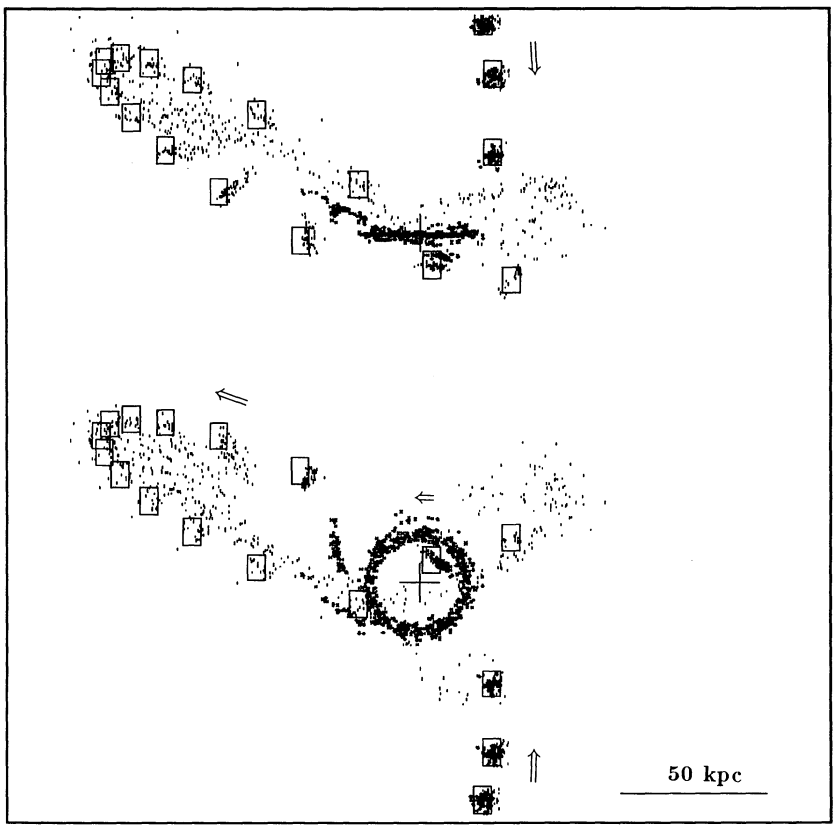

FIG. 8.—Prograde (direct) encounter for an initial condition $(x, y, z) = (0, -100, 100)$ kpc and $(v_x, v_y, v_z) = (+20, 0, -60)$ km s^{-1}. A ring is formed.

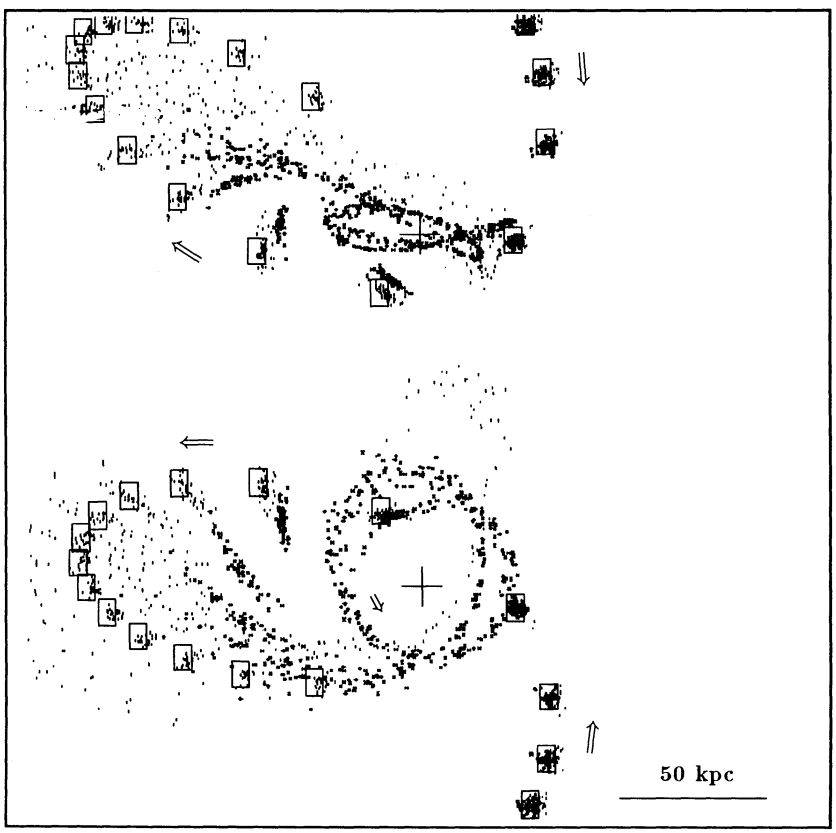

FIG. 9.—Prograde encounter for an initial condition $(x, y, z) = (0, -100, 100)$ kpc and $(v_x, v_y, v_z) = (+50, 0, 0)$ km s^{-1}. A ring of larger radius is formed. Also transient warped spiral arms appear in the outer region. Plot interval is 0.2 Gyr.

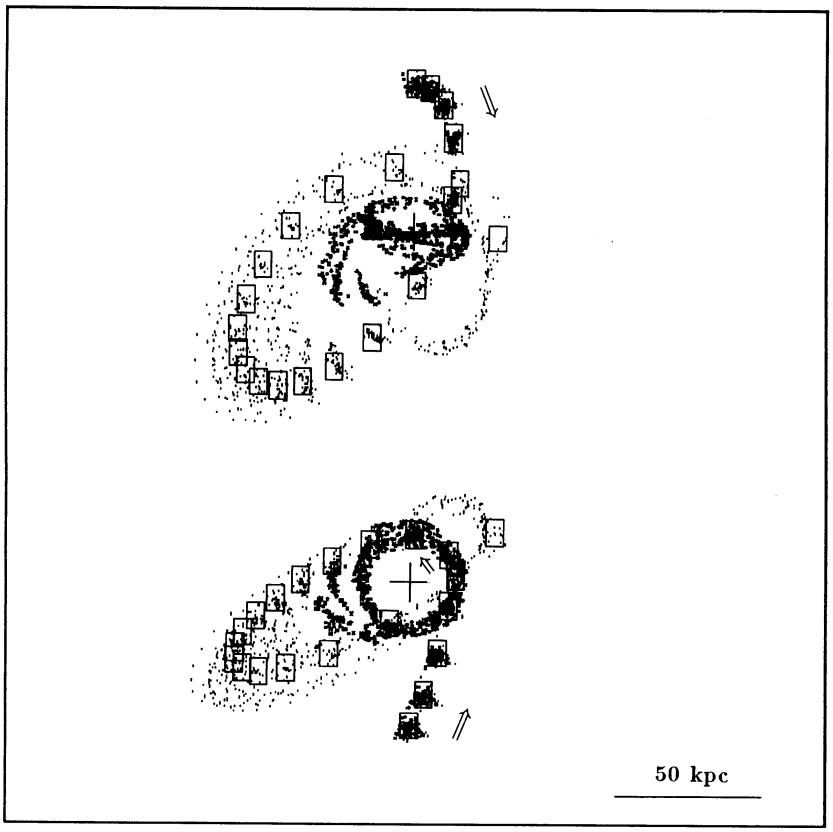

FIG. 10.—Prograde encounter for a closer orbit for an initial condition $(x, y, z) = (0, -50, 50)$ kpc and $(v_x, v_y, v_z) = (20, 50, 0)$ km s^{-1}. A ring is formed at a radius of 15 kpc.

for an initial condition in our simulation, because our interest is in the stripping process of their interstellar clouds, which we found to have occurred far before the orbit shrank to the present one by the dynamical friction. Hence, we apply the present ram-pressure stripping and accretion model to the past history of M32 several billion years ago, when its galactocentric distance was several tens of kiloparsecs.

4.1.2. *NGC 205*

The distance and radial velocity of NGC 205 are 640 kpc and -239 km s^{-1}, respectively, or the galaxy is at 30 kpc nearer position to us and is approaching M31 at a velocity of $+60$ km s^{-1} (see the literature cited above). Since NGC 205 lies in the plane defined by the line of sight and the minor axis [(y, z) plane], the probabilities of retrograde and prograde are the same. Here, we assume a polar orbit, as was assumed by Sato & Sawa (1986), who, however, put NGC 205 farther than M31. Cepa & Beckman (1988) also suggested a high-inclination retrograde orbit for NGC 205. Figures 6, 7 and 8 would simulate such a polar orbit case.

In the cases of both M32 and NGC 205, however, the determination of their actual orbits around M31 is still far from conclusive. We also mention the masses of the galaxies: the mass of M32 is around $5 \times 10^8\ M_\odot$ (Ford 1978; Byrd 1979) and that of NGC 205 around $10^{9\sim10}\ M_\odot$ (Sato & Sawa 1986), which are both smaller than the mass assumed for the companion used in the present simulation. However, if we consider that the companions have experienced tidal truncation of their outer mass during the past interactions with M31, it will be not unreasonable to assume larger masses in the simulation where they are assumed to still contain substantial amount of interstellar gas. Nevertheless, we should take the present result of simulation only as generic prediction what happened to gas clouds in these galaxies.

4.2. *Galaxy Merger in M31?*

Recently, the *Hubble Space Telescope* observations discovered a multiple nucleus in M31, which gives definite proof of the merger of substantial galaxies with M31 (Lauer et al. 1993). This fact implies that the gaseous stripping and accretion from companion galaxies took place not only from M32 and NGC 205, but also from another merged galaxy, which is now only seen as the second nucleus. Since it is also likely that the merger galaxy contained insterstellar gas, the present model applies also to this merger galaxy: The ram-pressure stripping must have occured when the merging galaxy rotated on an outer orbit, prior to the merging of the stellar body. The stripped gas will have been accreted by M31's disk along an accretion spiral, as simulated by the present models, and it must have behaved quite differently from the merger body's motion. Hence, the arguments given in the following subsections for the peculiar gaseous features in M31's bulge applies also to gaseous remnant during the merger.

4.3. *"Face-on Spirals" of Ionized and Molecular Gases in M31's Center*

As the simulation for retrograde encounter indicates, accreting clouds that hit the nuclear region exhibit peculiar kinematics, distinguished from the disk rotation, and this may explain some peculiar motions observed in the inner region of

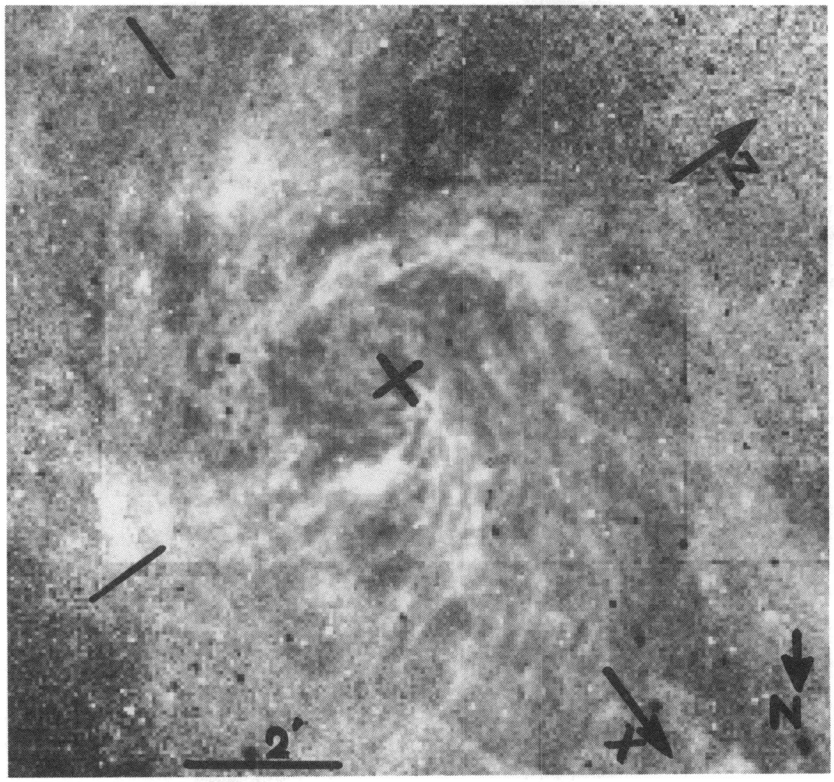

FIG. 11.—Hα image of the central 2 × 2 kpc region of M31 (reproduced from Ciardullo et al. 1988; courtesy of R. Ciardullo). A face-on spiral structure is seen in a good coincidence with the dark cloud feature in Fig. 12. The feature is reproduced qualitatively by the simulation as shown in Fig. 4.

M31. CCD imaging of the Hα emission of M31's bulge revealed peculiar spiral patterns of ionized gas and indicates an off-plane spirals which are rather "face-on" and exhibit anomalous velocities (Fig. 11: Ciardullo et al. 1988). By image processing and color excess analyses of *B*-, *V*-, *R*-, and *I*-band CCD images of the central region of M31, we also found a face-on spiral feature of dark clouds, which shows an excellent correlation with the Hα spirals (Fig. 12: Sofue et al. 1994). Although the central 1 kpc region exhibits such peculiar and prominent interstellar morphology, the gaseous mass itself is anomalously small (see § 4.4).

The spiral pattern as defined by the Hα emission and dark clouds is strongly asymmetric with respect to the galaxy center and appears one-armed and face-on. This face-on spiral has no connection with the major disk and spiral arms of M31 which are nearly edge-on at an inclination angle of 77°. In Figure 4*c* we showed the result of *N*-cloud simulation for the central region for the retrograde encounter. Except for scaling, the present simulation appears to nicely reproduce the observed characteristics of the peculiar spiral features in Figures 11 and 12. In this model, the dark clouds in the spiral are considered to be stripped clouds from the companion and/or merger galaxy, and the infalling motion and friction among the clouds may have heated them to be ionized so that they are observed in Hα.

Here, we compared our result with the observations only qualitatively. In order to obtain a better fitting to the observations, which reveal much narrower filamentary structures in the inner 1 kpc region, we need to investigate a more detailed accretion process properly simulating hydrodynamical behavior of individual clouds. Namely, we need to adopt a more realistic density distribution of the gas disk and take into account variation of cloud properties during interaction with the disk gas, as well as a change in the disk gas distribution itself.

Stripping and accretion occurs most efficiently when the companion crosses the galactic plane. Since the companions already rotated around M31 for several orbital periods, they should have encountered the M31 disk several times, and, accordingly, the stripping and accretion must have occurred recurrently for several times. The simulation indicates (Figs. 2–10) that molecular clouds infall more slowly than H I clouds do, because of their weaker ram braking, and, hence, molecular clouds can survive the accretion for more orbital rotations. It is, therefore, also possible that the observed peculiar features in M31's bulge are due to accretion of molecular clouds which were stripped some rotations ago. This will apply particularly for a merger in which the dynmical timescale is much shorter, and it happens that stripped clouds, particularly molecular clouds, fall into the nuclear region after the merger finished.

4.4. *Disruption of the Nuclear Gaseous Disk*

We have assumed that the disk gas in M31 has angular momentum large enough compared to that of infalling gas clouds. However, if we take into account the finite amount of angular momentum, the rotation, particularly that of the inner region, of the disk gas must be significantly affected by the accreting clouds (Sofue & Wakamatsu 1993). If the encounter is retrograde, the gas disk loses substantial amount of angular momentum, and, as a consequence, the gaseous disk shrinks and results in supplying the interstellar gas toward the nucleus. This process might have caused a sudden increase of dense gas in the nuclear region and triggered a starburst (Sofue & Wakamatsu 1991). The starburst would further cause a fast outflow

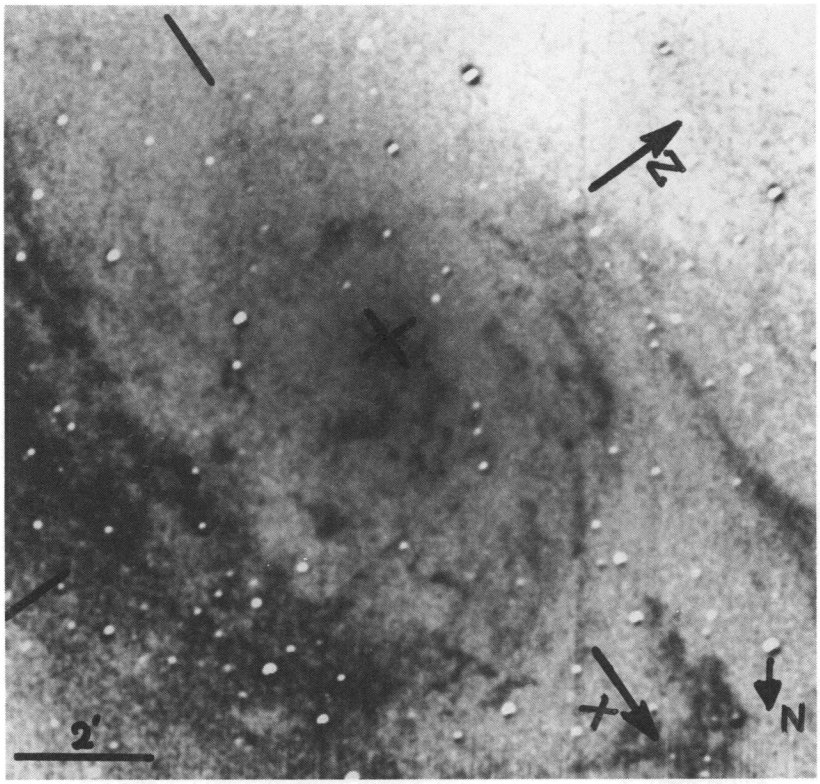

FIG. 12.—$B - V$ image of the central 2.4 kpc × 2.4 kpc region of M31, which was observed with the Kiso 105 cm Schmidt telescope (reproduced from Sofue et al. 1994). Dark clouds in the central 2 kpc are found to trace a face-on, one-armed spiral structure, which has no apparent connection with the major disk of M31, but comprises a disk perpendicular to M31's disk plane. The feature can be explained by the accretion spiral as simulated by the model shown in Fig. 4.

of interstellar gas due to energy injection by sudden enhancement of supernova explosions and stellar wind (e.g., Nakai et al. 1987) and will result in the disposal of gas from M31's bulge.

It will also happen that the vector of angular momentum changes significantly by the accretion of external gas clouds, and the inner disk becomes tilted from the original galactic plane. In fact, the central 1 kpc of M31's bulge exhibits almost face-on spiral arms as seen in Hα and in dark clouds (Ciardullo et al. 1988; Sofue et al. 1994), which might be a mixture of the accreted gas and disk gas.

Hence, the inner gaseous disk is disrupted and dissipated by infalling external gas clouds from the companions or the merger in such a way that it either shrinks toward the nucleus, expands to become a ring, or becomes tilted from the original plane. If a starburst occurs, it may also cause disposal of gas from the central region. This scenario can well explain why the central region of M31 contains little gas and shows early-type characteristics. In fact, observations show that the gaseous mass in the central 1 kpc is anomalously small, not exceeding some $10^7\ M_\odot$ (Brinks & Shane 1984; Koper et al. 1990; Allen & Lequeux 1993; Sofue & Yoshida 1993), which is one or two orders of magnitudes smaller compared to molecular gas mass in the central region of normal Sb galaxies like the Milky Way and NGC 891 (Sofue et al. 1987, 1993).

4.5. *The 10 Kiloparsec Gaseous Ring*

If the encounter is prograde or polar, as is possibly the case for clouds from NGC 205, the clouds' orbital angular momentum is added to the disk angular momentum, which results in expansion of the disk radius. Accordingly, the inner disk gas is accumulated on a gaseous ring at a larger radius. This will explain the 10 kpc ring of H I gas and a clear hole inside 8 kpc (Brinks & Shane 1984). This will also explain the large ring radius of molecular gas of about 10 kpc (Koper et al. 1991), which is anomalously large compared to molecular ring radii of 4–5 kpc observed in usual Sb galaxies such as the Galaxy (Dame et al. 1987) and NGC 891 (Sofue & Nakai 1993).

4.6. *Are M32 and NGC 205 Bulge Remnants of Disrupted Companions?*

The outer part of M32 is known to have been tidally cut off, and it would have lost a substantial fraction of the stellar disk (Nieto & Prugniel 1987). This implies that M32 may have possessed a larger disk with more gas in the past, but only the dense stellar bulge could have survived the tidal disruption. It would be, therefore, possible that M32 is a remnant of a bulge of a disrupted companion. This hypothesis explains the fact that M32 is anomalously compact and dense for its small mass (Nieto & Prugniel 1987) and hosts a compact nucleus (Richstone, Bower, & Dressler 1990), not like the usual dwarf ellipticals. Moreover, M32 has a surface brightness distribution which is more similar to that of a galactic bulge.

Another companion NGC 205 is known for its dark clouds (Sandage 1961) and interstellar hydrogen (Johnson & Gottesman 1983) as well as for a recent star-forming activity (Bica et al. 1990; Price & Grasdalen 1983). As our simulation shows, it is easy for clouds in a companion to be stripped. On the contrary, external clouds can hardly be captured by such a dwarf elliptical as NGC 205 during its orbital motion around a large disk galaxy like M31. The existence of interstellar gas in NGC 205 can be explained only by a remnant of interstellar gas which was originally contained in the galaxy. It is therefore

also possible that NGC 205 is a remnant of a bulge of a later type galaxy that contained more amount of gas in the past and possibly a disk.

5. DISCUSSION

We have performed test-cloud simulations of ram-pressure stripping and accretion of gas clouds from a companion galaxy onto its host galaxy. Obviously the result can be applied to systems of different scales by keeping the similarity among mass, length, and time. For example, without changing the masses, we can scale the length by a factor of f by scaling the time, velocity, and density by factors of $f^{3/2}$, $f^{-1/2}$, and f^{-3}, respectively. Although the simulation gives a generic behavior of clouds in interacting galaxy systems, we discussed particularly M31 and its companion as well as its possible merger galaxy.

We discuss below more general problems which would be related to the present model, and make some prediction based on this model.

5.1. *Disposal of Gas from Companions and One-Way Transfer*

Stripping and accretion of gas clouds from a companion to another galaxy should play a substantial role in their evolution. We stress that the gas transfer occurs much more rapidly than the stellar mass merger due to dynamical friction. The one-way transfer of gas results in a rapid evolution of the companion to become redder (gas poorer), and will lead to color contrast between the companion (redder) and its host (bluer). In fact, even just glancing at Arp's (1966) atlas of peculiar galaxies, we can find many multiple-galaxy systems in which the larger galaxy is of later type (spiral) and its companion is a dwarf elliptical or an early type such as a small S0. A typical example is seen for M51 (Sc) and its companion (dwarf elliptical irregular with a bar).

Ford (1978) showed that the gaseous mass observed in M32 is much less than that expected from the mass-loss rate from planetary nebulae and stressed that the disposal of mass lost from evolving stars in elliptical galaxies is an outstanding problem. An answer to this problem could be given by the present ram-pressure stripping model: such a small-mass companion as M32 ($\sim 5 \times 10^8\ M_\odot$) would be severely affected by ram stripping during its close encounter with the halo and disk of M31, resulting in an almost entire disposal of interstellar gas.

5.2. *Fate of Gaseous Debris: Magellanic Stream*

The dynamical evolution of the triple system of the Galaxy and the Large, and Small Magellanic Clouds has been extensively studied by numerical simulations (e.g., Fujimoto & Sofue 1976, 1977). In the current models of gravitational interaction, the Magellanic Stream (MS) of H I gas (Mathewson et al. 1979) has been reproduced as the tidal debris from the SMC disturbed mainly by the LMC and partly by the Galaxy. In these models, the H I debris were treated as test particles, and no hydrodynamical effect has been taken into account.

However, if we take into account the ram-pressure effect on the MS, it will rapidly infall toward the Galaxy and will be accreted by the galactic disk within about 1 Gyr. Since the orbit of the MC is nearly polar, the accreting gas will be merged by the rotating galactic disk at a radius of about 10 kpc.

We may convincingly conjecture that MS-like debris had been stripped rather recurrently during the past tidal interactions among the three galaxies. Hence, a greater number of MS-like clouds would be falling toward the Galaxy, some of which are already very close to the galactic plane or have merged. Infalling directions are not necessarily related to the orbit of the companion, but are polar spiral for a retrograde encounter, or they are in a semicorotation with the galactic disk for a prograde encounter. In either case, however, they are approaching the galactic disk and should be observed to have negative velocities when looked at from the Sun. Observed high-velocity H I clouds, which are accreting to the Galaxy at high negative velocities (e.g., van Woerden et al. 1985), could be understood to be such accreting clouds from companions.

5.3. *Fate of Gas during Merger*

Merger of galaxies has been numerically simulated using self-gravitating stellar systems (Barnes 1989). However, no particular analysis has been performed of the behavior of gaseous constituents during the merger. Since gas is not collisionless and more viscous compared to stars in dynamical interaction, gaseous constituents must interact more strongly. As the simulation indicated, the gas stripping and accretion occurs much faster than the dynamical merging timescale, even prior to merger starts.

If the perigalactic distance (or the impact parameter) is small enough and the companion encounters the central bulge of the host galaxy, the merger timescale must be much shorter. In such a case, the gas stripping will occur even at a large distance before the companion approaches the nucleus. However, the accretion of stripped clouds, particularly molecular clouds, takes place in a longer, or a comparable, timescale than the merging timescale. This implies that gaseous accretion would continue even after the merger has finished. In either case, orbits of stripped gas clouds are quite different from that of the stellar body. The gaseous merger during a galaxy merger will be subjected to a detailed analysis in a separate paper.

The author thanks R. Ciardullo for providing him with the Hα CCD image of M31's bulge. He is also indebted to the referee, G. G. Byrd, for valuable comments and suggestions to the manuscript.

REFERENCES

Allen, C. W. 1973, Astrophysical Quantities (London: Athlone), chap. 14
Allen, R. J., & Lequeux, J. 1993, ApJ, 410, L15
Arp, H. C. 1966, Atlas of Peculiar Galaxies (Pasadena: California Institute of Technology)
Barnes, J. E. 1989, Nature, 338, 123
Bica, E., Alloin, D., & Schmidt, A. A. 1990, A&A, 228, 23
Brinks, E., & Shane, W. W. 1984, A&A, 55, 179
Byrd, G. G. 1976, ApJ, 208, 688
———. 1977, ApJ, 218, 86
———. 1978, ApJ, 226, 70
———. 1979, ApJ, 231, 32
Cepa, J., & Beckman, J. E. 1988, A&A, 200, 21
Ciardullo, R., Rubin, V. C., Jacoby, G. H., Ford, H. C., & Ford, W. K., Jr. 1988, AJ, 95, 438
Dame, T. M., et al. 1987, ApJ, 322, 706
de Vaucouleurs G., de Vaucouleurs A., Corwin H. G., Jr., Buta, R. J., Paturel, G., & Fouqué, P. 1991, Third Reference Catalogue of Bright Galaxies (New York: Springer-Verlag)
Farouki, R., & Shapiro, L. 1980, ApJ, 241, 928
Ford, H. C. 1978, in IAU Symp. 76, Planetary Nebulae: Observations and Theory, ed. Y. Tersian (Dordrecht: Reidel), 19
Ford, H. C., Jacoby, G. H., & Jenner, D. C. 1978, ApJ, 208, 683
Fujimoto, M., & Sofue, Y. 1976, A&A, 47, 263
———. 1977, A&A, 61, 199

Johnson, D. W., & Gottesman, S. T. 1983, ApJ, 275, 549
Koper, E., Dame, T. M., Israel, F. P., & Thaddeus, P. 1991, ApJ, 383, L11
Kormendy, J. 1987, in Structure and Dynamics of Elliptical Galaxies, ed. T. de Zeeuw (Dordrecht: Reidel), 17
Lauer, T. 1993, AJ, in press
Mathewson, D. S., Ford, V. L., Schwarz, M. P., & Murray, J. D. 1979, in The Large-Scale Characteristics of the Galaxy, ed. W. B. Burton (Dordrecht: Reidel), 547
Miyamoto, M., & Nagai, R. 1975, PASJ, 27, 533
Murai, T., & Fujimoto, M. 1980, PASJ, 32, 581
Nakai, N., Hayashi, M., Handa, T., Sofue, Y., Hasegawa, T., & Sasaki, M. 1987, PASJ, 39, 685
Nieto, J. L., & Prugniel, P. 1987, in Structure and Dyanmics of Elliptical Galaxies, ed. T. de Zeeuw (Dordrecht: Reidel), 99
Price, J. S., & Grasdalen, G. L. 1983, ApJ, 275, 559
Richstone, D., Bower, G., & Dressler, A. 1990, ApJ, 353, 118
Sandage, A. 1961, The Hubble Atlas of Galaxies (Washington: Carnegie Institution of Washington), pl. 18
Sato, N. R., & Sawa, T. 1986, PASJ, 38, 63
Sofue, Y., & Nakai, N. 1993, PASJ, 45, 139
Sofue, Y., Nakai, N., & Handa, T. 1987, PASJ, 39, 47
Sofue, Y., & Wakamatsu, K. 1991, PASJ, 43, L57
———. 1992, PASJ, 44, L23
———. 1993, A&A, 273, 79
Sofue, Y., & Yoshida, S. 1993, ApJ, 417, L63
Sofue, Y., Yoshida, S., Aoki, T., Soyano, T., Tarusawa, K., & Wakamatsu, K. 1994, PASJ, in press
Toomre, A., & Toomre, J. 1972, ApJ, 178, 632
Tremaine, S. D. 1976, ApJ, 203, 72
van Woerden, H., Schwarz, U. J., & Hulsbosch, A. N. M. 1985, in The Milky Way Galaxy, ed. H. van Woerden & R. J. Allen (Dordrecht: Reidel), 387